# Model study of coherent quantum dynamics of hole states in functionalized semiconductor nanostructures

Luis G. C. Rego
*Department of Physics, Universidade Federal de Santa Catarina, Florianopolis, SC 88040-900, Brazil*

Sabas G. Abuabara and Victor S. Batista
*Department of Chemistry, Yale University, New Haven, Connecticut 06520-8107*

(Received 7 December 2004; accepted 25 January 2005; published online 19 April 2005)

Functionalization of semiconductor nanocrystals can be achieved by anchoring organic ligands to the surface dangling bonds. The resulting surface complexes often introduce electronic states in the semiconductor band gap. These interband states sensitize the host material for photoabsorption at frequencies characteristic of the molecular adsorbates, leading to the well-known process of photoexcitation and subsequent femtosecond interfacial electron transfer. This paper investigates the relaxation dynamics of hole states, energetically localized deep in the semiconductor band gap, after the ultrafast electron-hole pair separation due to interfacial electron transfer. Mixed quantum-classical methods, based on mean-field nuclear dynamics approximated by *ab initio* density functional theory molecular dynamics simulations, reveal superexchange hole tunneling between adjacent adsorbate molecules in a model study of functionalized $TiO_2$-anatase nanostructures. It is shown that electronic coherences can persist for hundreds of picoseconds under cryogenic and vacuum conditions, despite the partial intrinsic decoherence induced by thermal ionic motion, providing results of broad theoretical and experimental interest. © *2005 American Institute of Physics*. [DOI: 10.1063/1.1873712]

## I. INTRODUCTION

The ability to create and control, at the molecular level, electronic excitations in semiconductor materials is a subject of great interest for a wide range of fields, including nanotechnology,[1] microelectronics,[2] optoelectronics,[3] and imaging.[4] Organic functionalization of semiconductor surfaces can control for instance the growth of nanoparticles as well as their mechanical, electronic, and optical properties.[5,6] In particular, significant experimental[7–12] and theoretical[13–20] effort has been devoted to the study of $TiO_2$ functionalized semiconductors within the context of photoexcitation and subsequent interfacial electron transfer, including applications of these readily available materials to effective mechanisms of solar energy conversion.[21–26] This paper investigates the quantum relaxation dynamics of hole states, after electron-hole pair separation, in fully atomistic models of functionalized $TiO_2$-anatase nanostructures. Conditions that would naturally protect the evolution of quantum states against the decohering effect of thermal lattice motion are computationally investigated.

Surface complexes produced by organic functionalization often introduce electronic states in the semiconductor band gap (see energy diagram in Fig. 1). Such states sensitize the host material for photoabsorption at frequencies characteristic of the choice of molecular adsorbates. Photoexcitation of a surface complex results in ultrafast electron injection through electron-hole pair separation, so long as there exists a suitable energy match between the photoexcited molecular state in the adsorbate molecule and electronic states of similar symmetry in the conduction band of the semiconductor material.[10–12,17] The injected electron thermalizes in the conduction band, leaving a hole state localized in the surface complex. Under off-resonance conditions, relative to the semiconductor energy bands, the hole can relax only to the (usually discrete) subspace of near-resonant electronic states in neighboring adsorbate molecules coupled by the common host substrate, surface states, defects, or redox impurities (e.g., in a typical Grätzel cell the hole initially localized in an adsorbate molecule eventually relaxes to a nearby redox species in the surrounding electrolyte solution).

In pure semiconductors under vacuum conditions, where surface states are quenched by capping and functionalization of the surface dangling bonds, the off-resonance condition relative to the semiconductor energy bands confines the relaxation dynamics of hole states to near-resonant electronic states localized in the surface complexes (see energy diagram in Fig. 1). Such a relaxation dynamics is computationally investigated in this paper by using an approximate mixed quantum-classical approach (i.e., Ehrenfest mean-field nuclear dynamics), where the electrons are treated quantum mechanically and the nuclei evolve classically.

The loss of quantum coherence has been investigated in similar composite models, where a quantum subsystem is coupled to a buffer subsystem directly coupled to a thermal bath.[27] The applicability of mixed quantum-classical dynamics, where the buffer subsystem is treated classically, was found to be valid so long as the quantum subsystem decoheres slowly and the buffer quickly. Analogously, the computational models discussed in this paper involve decoherence of the electronic subsystem due to coupling with nuclear coordinates initially prepared at thermal equilibrium.

 

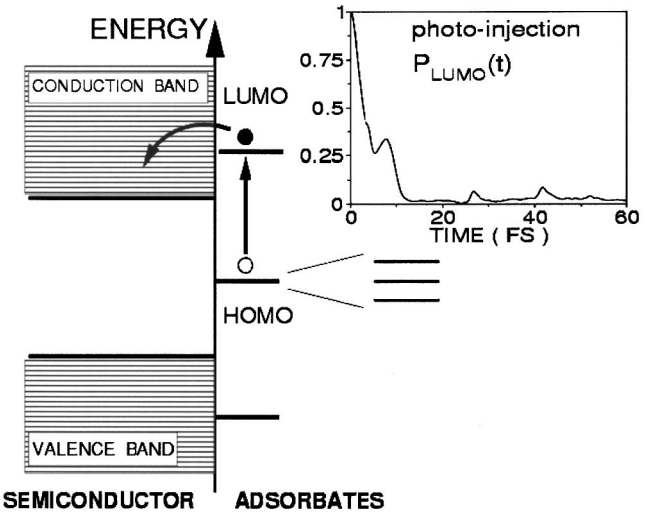


FIG. 1. Energy diagram of the model system discussed in Fig. 4. The scheme shows the energy levels of the adsorbates, including inhomogeneous broadening of the HOMO due to surface disorder, the HOMO→LUMO photoexcitation of a surface complex and the injection of a photoexcited electron into the conduction band of the semiconductor. The inset shows the LUMO time-dependent electron population reported in Ref. 14.

Of special interest is the persistence of electronic quantum coherences for long times, despite the partial deleterious effect induced by finite temperature ionic motion. It is important to note that the appreciation of conditions under which a quantum mechanical system may be approximated as a quantum-classical system has been the subject of intense research in recent years,[28–31] and the role of decoherence has been addressed in discussions of schemes for the simulation of condensed phase systems.[32,33]

The paper is organized as follows. Section II describes the catechol/$TiO_2$-anatase model system and the mixed quantum-classical simulation method. Details of the molecular dynamics calculations are discussed in Sec. II A. A description of the electronic Hamiltonian for the model system is included in Sec. II B. Section II C describes the simulations of hole relaxation dynamics. Results are presented and discussed in Sec. III. Section IV summarizes and concludes.

## II. METHODS

### A. Model system

The computational models are prepared according to previous studies of functionalized $TiO_2$ nanostructures.[17] The model system for molecular dynamics is composed of 32 $[TiO_2]$ units arranged according to the anatase crystalline structure,[34] functionalized with catechol adsorbed onto the (101) surface of the $TiO_2$-anatase crystal, and with dangling bonds on upper and lower surfaces capped with hydrogen atoms. Catechol is chosen as a prototype of aromatic anchoring ligands upon which a wide range of molecular structures could be attached for specific applications.[35] The surface dangling bonds are capped with hydrogen as part of conventional engineering orthodoxy to quench formation of surface states.[36]

The model is initially defined according to the unrelaxed anatase crystal structure. Representative configurations are obtained by geometry optimization and subsequent thermalization under conditions of 100 K and constant volume, using the Vienna *ab initio* simulation package (VASP/VAMP).[37] The VASP/VAMP package implements the density functional theory (DFT) in a plane-wave basis set, making use of the Perdew–Wang[38] generalized gradient approximation (GGA) for the exchange-correlation functional and ultrasoft Vanderbilt pseudopotentials for modeling the core electrons.[39] The Kohn–Sham (KS) Hamiltonian is projected onto a plane-wave basis set and high-efficiency interative methods are used to obtain the KS eigenstates and eigenvalues. Self-consistency is accelerated by means of efficient charge density mixing schemes. Calculations are performed with an SP2 supercomputer to take full advantage of the parallelized version of the code.

The preparation of the model system thus involves structural relaxation in response to functionalization.[13] These conformational changes and realignments also tend to quench the formation of surface states deep within the semiconductor band gap.[36] The phonon spectral density, obtained as the Fourier transform of the ionic velocity autocorrelation function, is consistent with previous calculations[13] as well as with the experimentally determined normal modes of $TiO_2$-anatase in the 262–876 $cm^{-1}$ range.[40] In addition, the 800–1600 $cm^{-1}$ frequency range corresponding to the catechol vibrational modes is found to be in good agreement with earlier studies.[41] The vibrational modes of $TiO_2$-anatase are expected to be only marginally affected by photoexcitation of the adsorbate molecule or electron injection into the conduction band. In addition, the ground-state vibrational frequencies of catechol molecules are only slightly affected by photoexcitation of the molecule to the S1 electronic state.[41] This implies similar nuclear motion (i.e., same vibrational frequency) regardless of changes of distinct character associated with the time-dependent electronic state.

### B. Electronic structure

Realistic simulations of interfacial electronic relaxation face the challenge of modeling quantum dynamics in rather extended model systems since finite size effects or even periodic boundary conditions can produce inaccurate results due to transient artificial electron population.[13] In addition, a reliable description of the electronic couplings between the discrete molecular states in the anchored molecules and the dense manifold of highly delocalized electronic levels in the semiconductor host substrate is required. To address these challenges, electronic relaxation is simulated in model nanoparticles constructed by the juxtaposition of three of the complex units described in Sec. II A extended along the $[-101]$ direction of the $TiO_2$-anatase structure (see Fig. 2), with periodic boundary conditions in the unextended direction. The resulting model systems correspond to experimentally realizable structures with dimensions $3.0\times1.5\times3.1$ $nm^3$ along the $[-101]$, $[010]$, and $[101]$ directions of the anatase crystal, respectively. These models contain a total of 372 atoms, including 96 $[TiO_2]$ units and three catechol molecules adsorbed on the (101) surface of a $TiO_2$-anatase nanostructure. For future reference, the central adsorbate

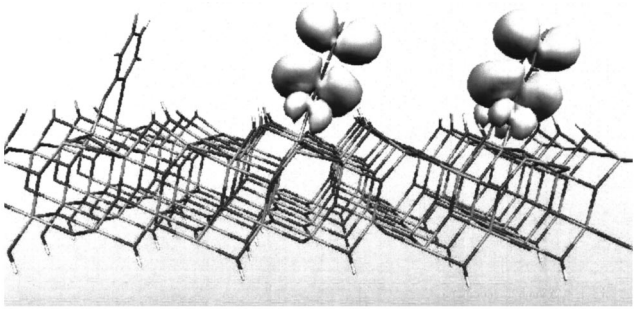

FIG. 2. $TiO_2$ nanostructure functionalized with catechol molecules and isodensity surface representing a time-evolved hole state localized simultaneously in two coupled molecular adsorbates.

molecule in the 3 nm particle is labeled *C* while the adsorbate molecules on the left and right are labeled *L* and *R*, respectively. Adjacent catechol molecules are 1 nm apart from each other, modeling a typical surface density of $\approx 1\ \mu\mathrm{mol/m}^2$.

The electronic structure of the 3 nm particles is described according to a tight-binding model Hamiltonian gained from the extended Hückel (EH) approach.[42,43] Advantages of this method are that it requires a relatively small number of transferable parameters and is capable of providing accurate results for the energy bands of elemental materials (including transition metals) as well as compound bulk materials in various phases.[43] In addition, the EH method is applicable to large extended systems and provides valuable insight on the role of chemical bonding.[44] The EH method is therefore most suitable to develop a clear chemical picture of the underlying relaxation dynamics at the semiquantitative level, including fundamental insight on the role that symmetry plays in the localization of holes on catechol molecular orbitals (MOs) (i.e., states with negligible overlap with *d* orbitals of nearby $Ti^{4+}$ ions in the $TiO_2$ host substrate).

The EH Hamiltonian is computed in the basis of Slater-type orbitals $\chi$ for the radial part of the atomic orbital (AO) wave functions,[13] including the 4s, 4p, and 3d atomic orbitals of $Ti^{4+}$ ions, the 2s and 2p atomic orbitals of $O^{2-}$ ions, the 2s and 2p atomic orbitals of C atoms, and the 1s atomic orbitals of H atoms. The AOs $\{|\chi_i(t)\rangle\}$ form a mobile (nonorthogonal) basis set due to nuclear motion, with $S_{ij}(t)=\langle\chi_i(t)|\chi_j(t)\rangle$ the corresponding time-dependent overlap matrix elements. The overlap matrix is computed using the periodic boundary conditions along the [010] direction.

Diagonalization of the EH Hamiltonian predicts a 3.3 eV band gap for the 3.0 nm model system in its relaxed configuration. This result is consistent with the experimental value of 3.2 eV for the band gap of bulk $TiO_2$-anatase, 3.4 eV for 2.4 nm particles[45] and 3.7 eV band gap for the 1.2 nm model system,[13] since the smaller the nanoparticle is the larger the band gap.

### C. Hole relaxation dynamics

We confine ourselves to an approximate mixed quantum-classical method in which the electrons are treated quantum mechanically and the nuclei classically. The nuclei evolve on an effective mean-field Born–Oppenheimer potential energy surface (PES), $V_{\mathrm{eff}}$, according to classical trajectories $\mathbf{R}^{\xi}=\mathbf{R}^{\xi}(t)$ with initial conditions specified by the index $\xi$. The time-dependent electronic wave function is propagated for each nuclear trajectory $\mathbf{R}^{\xi}(t)$, according to a numerically exact integration of the time-dependent Schrödinger equation (TDSE),

$$\left\{\frac{\partial}{\partial t}+\frac{i}{\hbar}\mathbf{H}(t)\right\}|\Psi^{\xi}(t)\rangle=0. \tag{1}$$

Here, $\mathbf{H}(t)$ is the electronic EH Hamiltonian described in Sec. II B which depends on *t* through $\mathbf{R}^{\xi}(t)$. The actual calculation of $V_{\mathrm{eff}}$, or equivalently of the set of trajectories $\mathbf{R}^{\xi}(t)$, is a difficult problem.[46] However, in the present application both the ground and excited electronic state PESs involve bound nuclear motion of similar frequencies. Therefore, $V_{\mathrm{eff}}$ is nearly parallel to the ground state PES. Nuclear trajectories $\mathbf{R}^{\xi}(t)$ are therefore approximated according to *ab initio*-DFT molecular dynamics simulations. Results reported in Sec. III are obtained, according to the resulting approximate propagation scheme, by sampling initial conditions $\xi$ for nuclear motion, integration of the TDSE over the corresponding nuclear trajectories and averaging expectation values over the resulting time-evolved wave functions. Converged results are typically obtained with less than 50 initial conditions representing the system thermalized under conditions of 100 K and constant volume. However, results are reported for averages of 100 initial conditions.

The TDSE, introduced by Eq. (1), is numerically integrated by expanding the time-dependent hole wave function $|\Psi^{\xi}(t)\rangle$ in the basis of the instantaneous MOs $|\phi_q(t)\rangle=\Sigma_i C_{i,q}(t)|\chi_i(t)\rangle$—i.e., the instantaneous eigenstates of the generalized eigenvalue problem $\mathbf{H}(t)\mathbf{C}(t)=\mathbf{S}(t)\mathbf{C}(t)\mathbf{E}(t)$, with eigenvalues $E_q(t)$,

$$|\Psi^{\xi}(t)\rangle=\sum_q B_q(t)|\phi_q(t)\rangle. \tag{2}$$

The propagation scheme is based on the recursive application of the following short-time approximation:

$$|\Psi^{\xi}(t+\tau/2)\rangle\approx\sum_q B_q(t)e^{-(i/\hbar)E_q(t)\tau/2}|\phi_q(t)\rangle, \tag{3}$$

where the evolution of the expansion coefficients

$$B_q(t+\tau)=\sum_p B_p(t)e^{-(i/\hbar)[E_p(t)+E_q(t+\tau)]\tau/2}\times\langle\phi_q(t+\tau)|\phi_p(t)\rangle \tag{4}$$

is approximated as follows:

$$B_q(t+\tau)\approx B_q(t)e^{-(i/\hbar)[E_q(t)+E_q(t+\tau)]\tau/2}, \tag{5}$$

in the limit of sufficiently thin time-slices $\tau$.

The initial hole state, after electron-hole pair separation, is the highest occupied molecular orbital (HOMO) of the initially photoexcited surface-complex *C*. The subsequent relaxation dynamics is quantitatively described in terms of the time-dependent hole population $\mathbf{P}_{\Omega}(t)$ of molecular adsorbate $\Omega=(L,C,R)$.

The time-dependent hole population $\mathbf{P}_{\Omega}(t)$ is computed as follows:

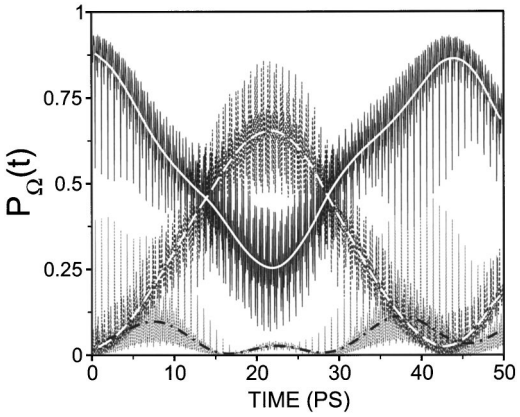


FIG. 3. Time-dependent hole population of adsorbate molecules $\Omega=(C, R, L)$ in thick white-solid, white-dashed, and black-dot-dash lines, respectively. Superimposed thin solid lines show the contribution of a single representative trajectory to the total ensemble average populations $\mathbf{P}_\Omega(t)$.

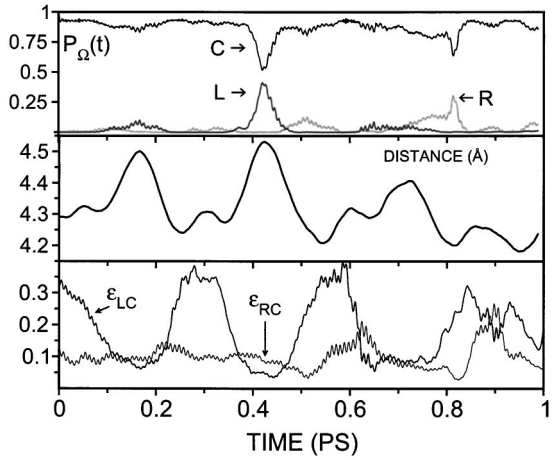


FIG. 4. Upper panel, time-dependent hole population $\mathbf{P}_\Omega(t)$ of adsorbate molecules: $\Omega=C$ and $\Omega=L$ (top and bottom black lines, respectively), and $\Omega=R$ (gray line). Middle panel, adsorbate-semiconductor distance measured from the center of mass of catechol to the semiconductor surface. Lower panel, energy difference (in meV) between near-resonant MOs.

$$\mathbf{P}_\Omega(t) = \mathrm{Tr}\{\hat{\rho}(t)\hat{P}_\Omega\}, \tag{6}$$

where $\hat{P}_\Omega$ is the projection operator onto atomic orbitals of adsorbate $\Omega$,

$$\hat{P}_\Omega = \sum_{k,j\in\Omega} |\chi_j\rangle S^{-1}_{jk}\langle\chi_k|, \tag{7}$$

and $\hat{\rho}(t)$ is the reduced density operator associated with the electronic degrees of freedom,

$$\hat{\rho}(t) = \sum_\xi p_\xi |\Psi^\xi(t)\rangle\langle\Psi^\xi(t)|, \tag{8}$$

where $p_\xi$ is the probability of sampling the nuclear initial condition specified by index $\xi$.

## III. RESULTS AND DISCUSSION

Figure 3 shows the evolution of the time-dependent population $\mathbf{P}_\Omega(t)$, with $\Omega=(L,C,R)$, during the first 50 ps of dynamics (thick lines). The thin lines in Fig. 3 illustrate the contributions of a single representative trajectory $\mathbf{R}^\xi$ to the total ensemble averages $\mathbf{P}_\Omega(t)$. Note that almost 90% of the hole population remains localized, throughout the entire relaxation time, on those atomic orbitals belonging to the adsorbate molecules. The remaining 10% of the hole population remains next to the molecular adsorbates, localized in the d orbitals of $Ti^{4+}$ ions that have partial overlap with the molecular adsorbates.

Figure 3 indicates that the hole is transferred between adjacent catechol molecules, remaining localized in the mono-layer of adsorbate molecules rather than undergoing injection into the semiconductor host substrate. The underlying hole relaxation dynamics is therefore significantly different from the relaxation of the photoexcited electron which, according to the results reported in Refs. 13 and 14 as well as in the inset of Fig. 1, is usually completely injected into the semiconductor material within a few femtoseconds.

Note that hole transfer involves *tunneling* between adjacent molecular adsorbates, since adsorbates are anchored to the semiconductor surface more than 1 nm away and therefore there is no significant overlap between the AOs of nearby adsorbate molecules. However, near-resonant electronic states, localized in adjacent adsorbate molecules, are indirectly coupled by the common semiconductor host structure. The results shown in Fig. 3, therefore, are consistent with a superexchange hole transfer mechanism mediated by the semiconductor host substrate.

An approximate description of hole tunneling between adsorbate molecules $\Omega$ and $\Omega'$, coupled by the host substrate, can be given in terms of the Rabi formulas: $\mathbf{P}_\Omega(t) = (\gamma^2_{\Omega\Omega'}/\hbar^2)/\Gamma^2_{\Omega\Omega'}\sin^2(\Gamma_{\Omega\Omega'}t)$ and $\mathbf{P}_{\Omega'}(t)=1-\mathbf{P}_\Omega(t)$. The calculated hole-tunneling period, obtained from Fig. 3, is T $\approx$ 42 ps and has an exponential dependence with the separation between molecular adsorbates. The parameter $\Gamma_{\Omega\Omega'} = [(\gamma_{\Omega\Omega'}/\hbar)^2+(\omega_{\Omega\Omega'}/2)^2]^{1/2}$ is the Rabi frequency, $\gamma_{\Omega\Omega'}$ is the effective quantum coupling between resonant states and $\omega_{\Omega\Omega'}$ is the corresponding Bohr frequency. The parameters computed from Fig. 3 are $\omega_{LC}\approx 4.5\,\omega_{RC}$ and $\gamma_{RC} \approx 1.12\,\gamma_{LC}$. It is important to mention that the asymmetric nature of the underlying relaxation dynamics (as evidenced by the asymmetric population of the $R$ and $L$ adsorbates) is primarily due to the intrinsic asymmetry of the substrate environments that interact with the adsorbates. Such small differences in local environments determine asymmetric couplings between molecular adsorbates and a preferential direction for the hole motion.

Figure 4 shows a detailed analysis of the early time relaxation dynamics for a representative nuclear trajectory, including the quantitative description of the adsorbate time-dependent hole population, the evolution of the adsorbate-semiconductor distance, and the evolution of energy differences between near-resonant electronic states of surface complexes localized in the semiconductor band gap.

Figure 4 shows that the time-dependent populations $\mathbf{P}_\Omega(t)$ (top panel) are correlated with the motion of the molecular adsorbates (middle panel), since the adsorbate-semiconductor separation modulates the time-dependent energy differences $\varepsilon_{RC}$ and $\varepsilon_{LC}$ between the initially populated state $C$ and the near-resonant electronic states in the $R$ and $L$

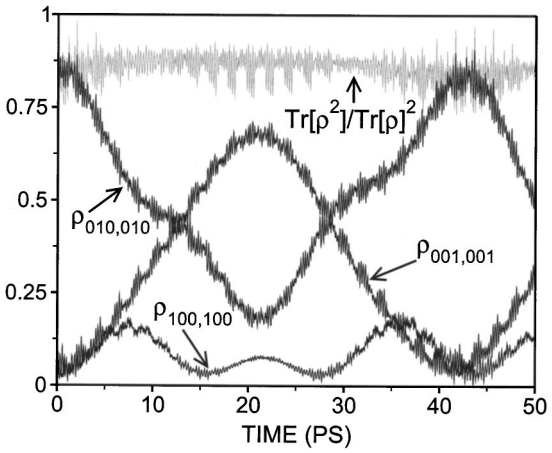


FIG. 5. Comparison of the trace of the square of the reduced density matrix (gray curve) and the time evolution of the hole population on the surface complexes *L*, *C*, *R* (black curves). Ensemble averages were converged by sampling over 100 different initial conditions $\xi$.

adsorbates, respectively (bottom panel). The maximum population exchange during this first picosecond of dynamics is observed when the adsorbate-semiconductor separation reaches a maximum value, at $\approx t=0.42$ ps. These results indicate that moderate thermal fluctuations can exert a strong influence on the hole relaxation dynamics by modulating the resonance condition and the electronic couplings between the electronic states responsible for hole transfer.

The extent to which these results are significant is associated with the survival of electronic coherences, responsible for the Rabi oscillations shown in Fig. 3. To this end, we examine the diagonal and off-diagonal elements of the reduced density matrix $\rho(t)$, introduced by Eq. (8), in the basis of catechol MOs. The analysis, presented in Figs. 5 and 6 is focused on the matrix elements of the HOMOs of isolated catechol molecules *L*, *C*, and *R*, which can be represented in occupancy notation as register states $|100\rangle$, $|010\rangle$, and $|001\rangle$, respectively. Note that in this notation $\hat{\rho}(0)=|010\rangle\langle 010|$.

The black curves in Fig. 5 show that the diagonal elements of the reduced density matrix for states $|100\rangle$, $|010\rangle$, and $|001\rangle$ correspond closely with the total adsorbate populations $\mathbf{P}_L(t)$, $\mathbf{P}_C(t)$, and $\mathbf{P}_R(t)$ reported in Fig. 3, indicating that most of the hole population remains localized in these adsorbate states throughout the simulation time. Furthermore, the nonzero off-diagonal elements, shown in Fig. 6, demonstrate that the hole relaxation dynamics remains remarkably coherent for the entire simulation time despite thermal nuclear motion. (Note: For clarity, results are presented for the first 50 ps of dynamics. It is, however, important to mention that our calculations indicate that both Rabi oscillation and quantum coherences are preserved for at least hundreds of picoseconds.)

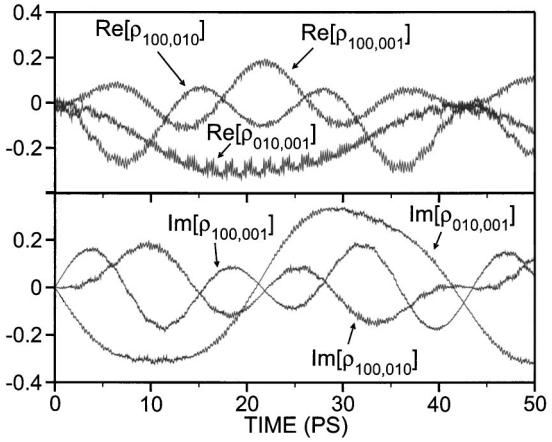


FIG. 6. Real (upper panel) and imaginary (lower panel) parts of nonzero off-diagonal matrix elements of reduced density matrix for register states $|100\rangle$, $|010\rangle$, and $|001\rangle$ demonstrating coherent superexchange hole tunneling dynamics for the first 50 ps of dynamics.

The observed coherent localization in the space of electronic states is mainly due to the finite size of the nanostructure, where the register states are coupled by the common host substrate but remain off-resonant relative to valence and conduction bands (manifolds) of electronic states.[13] In contrast, the analogous relaxation dynamics on extended systems is expected to delocalize the hole excitation on the manifold of near-resonant electronic states introduced by the adsorbate molecules. Hole excitations in disordered extended systems with low surface coverage, however, are expected to have an intermediate behavior and exhibit localized coherent relaxation within small disjoint islands of adsorbate molecules.

A quantitative measure of intrinsic decoherence is obtained by computing the trace of the square of the reduced density matrix $\mathrm{Tr}[\rho^2(t)]$.[47–49] Such a quantity measures the decay of purity as the initial state becomes a statistical mixture of electronic states due to the decoherence induced by thermal nuclear motion. (Note: We refer to the decoherence induced by the nuclear motion on the quantum subsystem as *intrinsic decoherence* to make a distinction from cases where decoherence is caused by the direct coupling of the quantum subsystem to an external bath.)

The gray curve in Fig. 5 shows that $\mathrm{Tr}[\rho^2(t)]$ decays about 15% at very early times due to partial mixing in the initially photoexcited surface complex *C*. However, $\mathrm{Tr}[\rho^2(t)]$ remains approximately constant throughout the rest of the propagation time, decaying at a much lower rate while the hole tunnels between adjacent molecular adsorbates. These results indicate that the underlying hole relaxation dynamics remains highly coherent on the surface of the nanoparticle in spite of thermal nuclear motion.

## IV. CONCLUSIONS

We have shown that mixed quantum-classical simulations, based on *ab initio*-DFT molecular dynamics, reveal the feasibility of superexchange hole tunneling dynamics in a model study of functionalized $TiO_2$-anatase nanostructure under cryogenic and vacuum conditions.

We have shown that quantum coherences between hole states, localized energetically deep in the semiconductor band gap, can persist for hundreds of picoseconds, despite the partial intrinsic decoherence induced by thermal ionic motion, providing results of broad theoretical and experimental interest. The observed coherent hole population transfer among adjacent adsorbates is mainly stabilized by the

finite size of the nanostructure, where the register states are coupled by the common host substrate but remain off-resonant relative to the valence and conduction bands (manifolds) of electronic states. Carrier-phonon, and likely carrier-carrier, scattering mechanisms are, therefore, highly suppressed by the off-resonance and symmetry conditions of the electronic states in surface complexes. Such processes would otherwise lead to the commonly observed ultrafast decoherence in semiconductor spectroscopy.[50,51]

We have suggested that the observation of Rabi oscillations, associated with the adsorbate electronic populations, could provide a simple experimental probe of the predicted coherent quantum relaxation dynamics. Considering the great technological interest in encoding and manipulating quantum states we anticipate significant experimental interest in examining the predicted relaxation dynamics reported in this paper.

In a subsequent investigation motivated by these results, we examine the feasibility of coherently controlling the underlying hole relaxation dynamics.[52] The results reported therein suggest that functionalized $TiO_2$ semiconductor materials might offer a readily available platform to encode logical hole states within the subspace of adsorbate surface complexes, where symmetry and off-resonance properties naturally provide a passive error prevention scheme,[53] protecting the evolution of quantum states against the decoherence effect of the lattice motion.

## ACKNOWLEDGMENTS

L.G.C.R. acknowledges financial support from CAPES/Brazil, under the PRODOC program. V.S.B. acknowledges supercomputer time from the National Energy Research Scientific Computing (NERSC) Center and financial support from Research Corporation, Research Innovation Award No. RI0702, a Petroleum Research Fund Award from the American Chemical Society Grant No. PRF 37789-G6, a junior faculty award from the F. Warren Hellman Family, the National Science Foundation (NSF) Career Program Award No. CHE 0345984, the NSF Nanoscale Exploratory Research (NER) Award No. ECS 0404191, and start-up package funds from the Provost's office at Yale University.

[1] J. Schoonman, Solid State Ionics **135**, 5 (2000).
[2] K. Vydianathan, G. Nuesca, G. Peterson, E. Eisenbraun, A. Kaloyeros, J. Sullivan, and B. Han, J. Mater. Res. **16**, 1838 (2001).
[3] Z. Wang, J. Phys.: Condens. Matter **16**, R829 (2004).
[4] K. Jacobson and R. Jacobson, *Imaging Systems* (Wiley, New York, 1976).
[5] S. Bent, Surf. Sci. **500**, 879 (2002).
[6] N. Pesika, Z. Hu, K. Stebe, and P. Searson, J. Phys. Chem. B **106**, 6985 (2002).
[7] D. Wheeler, J. Rodriguez, and J. McCusker, J. Phys. Chem. A **103**, 4101 (1999).
[8] Y. Liu, J. Dadap, D. Zimdars, and K. Eisenthal, J. Phys. Chem. B **103**, 2480 (1999).
[9] D. P. G. Ramakrishna, A. K. Singh, and H. Ghosh, J. Phys. Chem. B **108**, 1701 (2004).
[10] J. Schnadt, P. Bruhwiler, L. Patthey *et al.*, Nature (London) **418**, 620 (2002).
[11] J. Schnadt, J. O'Shea, L. Patthey *et al.*, J. Chem. Phys. **119**, 12462 (2003).
[12] J. Asbury, E. Hao, Y. Wang, H. Ghosh, and T. Lian, J. Phys. Chem. B **105**, 4545 (2001).
[13] L. G. C. Rego, S. G. Abuabara, and V. S. Batista, J. Am. Chem. Soc. **125**, 7989 (2003).
[14] L. G. C. Rego, S. G. Abuabara, and V. S. Batista, J. Am. Chem. Soc. (to be submitted).
[15] S. Ramakrishna, F. Willig, V. May, and A. Knorr, J. Phys. Chem. B **107**, 607 (2003).
[16] W. Stier and O. Prezhdo, J. Phys. Chem. B **106**, 8047 (2002).
[17] W. Stier and O. Prezhdo, J. Mol. Struct.: THEOCHEM **630**, 33 (2003).
[18] B. Smith and A. Nozik, J. Phys. Chem. B **103**, 9915 (1999).
[19] B. Smith and A. Nozik, J. Chem. Phys. **205**, 47 (1996).
[20] I. K. M. Thoss and H. Wang, Chem. Phys. **304**, 169 (2004).
[21] R. Miller, G. McLendon, A. Nozik, F. Willing, and W. Schmickler, *Surface Electron-Transfer Processes* (VCH, New York, 1995).
[22] A. Nozik and R. Memming, J. Phys. Chem. **100**, 13061 (1996).
[23] A. Gratzel, Chem. Rev. (Washington, D.C.) **95**, 49 (1995).
[24] P. Kamat and D. Meisel, *Semiconductor Nanocluster-Physical, Chemical, and Catalytic Aspects* (Elsevier, Amsterdam, 1997).
[25] E. M. C. Bauer, G. Boschloo, and A. Hagfeldt, J. Chem. Phys. **106**, 12693 (2002).
[26] A. Gratzel, Acc. Chem. Res. **33**, 269 (2000).
[27] K. Shiokawa and R. Kapral, J. Chem. Phys. **117**, 7852 (2002).
[28] W. Zurek, Phys. Rev. D **24**, 1516 (1981).
[29] W. Zurek, Phys. Rev. D **26**, 1862 (1981).
[30] E. Joos and H. Zeh, Z. Phys. B: Condens. Matter **59**, 223 (1985).
[31] E. Joos, H. Zeh, C. Kiefer, D. Giulini, J. Kupsch, and I.-O. Stamatescu, *Decoherence and the Appearance of a Classical World in Quantum Theory* (Springer, Berlin Heidelberg, 1996).
[32] E. Bittner and P. Rossky, J. Chem. Phys. **103**, 8130 (1995).
[33] O. Prezhdo and P. Rossky, Phys. Rev. Lett. **81**, 5294 (1998).
[34] A. Vittadini, A. Selloni, F. Rotzinger, and M. Gratzel, J. Phys. Chem. B **104**, 1300 (2000).
[35] C. Rice, M. Ward, M. Nazeeruddin, and M. Gratzel, New J. Chem. **24**, 651 (2000).
[36] W. Mönch, *Semiconductor Surfaces and Interfaces* (Springer, Berlin, 1993).
[37] G. Kresse and J. Furthmuller, Phys. Rev. B **54**, 11169 (1996), http://cms.mpi.univie.ac.at/vasp/
[38] J. Perdew, in *Electronic Structure of Solids*, edited by P. Ziesche and H. Eschrig (Akademie, Berlin, 1991).
[39] K. Laasonen, A. Pasquarello, R. Car, and C. Lee, Phys. Rev. B **47**, 10142 (1993).
[40] R. Gonzalez and R. Zallen, Phys. Rev. B **55**, 7014 (1997).
[41] M. Gerhards, W. Perl, S. Schumm, U. Henrichs, C. Jacoby, and K. Kleinermanns, J. Chem. Phys. **104**, 972 (1996).
[42] S. Glynn, L. Vanquickenborne, M. Kinoshita, and D. Carroll, in *Introduction to Applied Quantum Chemistry*, edited by Holt (Rinehart and Winston Inc., New York, 1972).
[43] J. Cerda and F. Soria, Phys. Rev. B **61**, 7965 (2000).
[44] R. Hoffmann, Rev. Mod. Phys. **60**, 601 (1988).
[45] D. B. C. Korman and M. Hoffman, J. Phys. Chem. **92**, 5196 (1998).
[46] P. Pechukas, Phys. Rev. **181**, 166 (1969).
[47] S. Flores and V. Batista, J. Phys. Chem. B **108**, 6745 (2004).
[48] V. Batista and P. Brumer, Phys. Rev. Lett. **89**, 143201 (2002).
[49] S. Habib, W. Zurek, and J. Paz, Phys. Rev. Lett. **70**, 1187 (1993).
[50] V. Axt and T. Kuhn, Rep. Prog. Phys. **67**, 433 (2004).
[51] U. Hohenester, F. Troiani, E. Molinari, G. Panzarini, and C. Macchiavello, Appl. Phys. Lett. **77**, 1864 (2000).
[52] L. G. C. Rego, S. G. Abuabara, and V. S. Batista, Quantum. Inform. Compu. (submitted).
[53] P. Zanardi and M. Rasetti, Mod. Phys. Lett. B **11**, 1085 (1997).